

# Prediction of Entropy Production and Heat Transfer Characteristics of $\text{Al}_2\text{O}_3\text{-Cu}$ /Water Hybrid Nanofluid in Convection-Radiation Interaction Flow in a Porous Cavity by Machine Learning Approach

Andaç Batur Çolak\*

Department of Information Systems and Technologies, Faculty of Computer and Information Sciences, Nigde Omer Halisdemir University, Nigde, 51240, Türkiye

## INFORMATION

### Keywords:

Entropy production  
heat transfer characteristics  
convection-radiation interaction  
porous cavity  
artificial neural network

DOI: 10.23967/j.rimni.2025.10.71901

Revista Internacional  
Métodos numéricos  
para cálculo y diseño en ingeniería

RIMNI



UNIVERSITAT POLITÈCNICA  
DE CATALUNYA  
BARCELONATECH

In cooperation with  
CIMNE<sup>3</sup>

## Prediction of Entropy Production and Heat Transfer Characteristics of $\text{Al}_2\text{O}_3$ -Cu/Water Hybrid Nanofluid in Convection-Radiation Interaction Flow in a Porous Cavity by Machine Learning Approach

Andaç Batur Çolak<sup>\*</sup>

Department of Information Systems and Technologies, Faculty of Computer and Information Sciences, Nigde Omer Halisdemir University, Nigde, 51240, Türkiye

### ABSTRACT

Minimizing entropy production is critically important, particularly in nanofluid flows. Applying this principle to flows with porous cavity structures helps optimize heat transfer applications and enhance system efficiency. In this study, the entropy production and heat transfer characteristics of a hybrid nanofluid composed of  $\text{Al}_2\text{O}_3$ -Cu particles suspended in water were investigated using machine learning. The nanofluid was analyzed in the context of convection–radiation interaction flow within a porous cavity. An artificial neural network model was developed to predict the average Nusselt number, Bejan number, and entropy production as functions of the Hartmann number and inclination parameters. The Bayesian Regularization algorithm was employed to train the multilayer perceptron network model. Prediction results obtained from the model with 10 neurons in the hidden layer were compared with the target values and showed excellent agreement. The developed artificial neural network model successfully predicted the Nusselt number, Bejan number, and entropy production with average deviation rates of  $-0.007\%$ ,  $-0.11\%$ , and  $0.0002\%$ , respectively.

### OPEN ACCESS

**Received:** 14/08/2025

**Accepted:** 30/09/2025

**Published:** 03/02/2026

### DOI

10.23967/j.rimni.2025.10.71901

### Keywords:

Entropy production  
heat transfer characteristics  
convection-radiation interaction  
porous cavity  
artificial neural network

### Nomenclature

ANN	Artificial neural network
Be	Bejan number
Ha	Hartmann number
MoD	Margin of deviation (%)
MSE	Mean square error
MWCNT	Multi-Walled carbon nanotube
Nu	Nusselt number
R	Coefficient of determination
S	Entropy generation
SWCNT	Single-Walled carbon nanotube

## Symbols

$\Phi$                     Inclination

## Subscripts

av                    Average  
pred                Prediction  
targ                Target

## 1 Introduction

Nanofluids, which are one of the heat transfer fluids that provide higher thermal performance, are used in various cooling applications such as electronic cooling [1], automotive [2], the food industry [3], solar energy applications [4], the petroleum industry [5], medicine [6] and heating and ventilation [7]. Examining the formation of entropy is a significant concern when studying heat transmission methods. Bejan [8] initially introduced the notion of entropy generation and its practical uses. Entropy is produced during irreversible events in the fluid flow domain, which reduces the efficiency of thermal equipment. The performance of thermal equipment relies on minimizing entropy formation and optimizing heat transport. Furthermore, the effectiveness of thermal equipment is contingent upon its cooling efficiency. Studies on nanofluids generally focus on issues such as determining thermophysical properties, improving heat transfer and increasing efficiency. In addition, there are some studies on the entropy production of nanofluids. In their study, Jiang et al. [9] conducted a simulation of the flow of a hybrid nanofluid consisting of Fe<sub>3</sub>O<sub>4</sub>/MWCNT particles suspended in water within a three-dimensional cubic enclosure. The enclosure was filled with a porous media. The flow region was presumed to consist of two revolving cylinders and include an undulating upper wall. In addition, the magnetic field was employed to address the issue arising from the presence of magnetic nanoparticles in the water. The Galerkin finite element method was utilized to solve the governing equations, employing triangular elements. The results were demonstrated for several flow parameters, including the angular velocity of the cylinder, Hartmann number, Darcy number, and the direction and position of the cylinders' rotations within the cavity. The impact of different factors on flow, heat transport, and entropy production was demonstrated through the use of the stream function, isotherms, and isentropic contours. Increased values of the Damkohler number and decreased values of the Hartmann number resulted in improved heat transport and higher Nusselt numbers. The main cause of entropy formation was heat transfer, although fluid-friction and magneto effects also made significant contributions.

In their study, Al-Amir et al. [10] examined the phenomenon of entropy production and natural convection in a Z-staggered cavity that was filled with porous media and a nanofluid consisting of TiO<sub>2</sub> particles dispersed in water. The possibility of using symmetrical enclosures was taken into consideration, and the media consisted of a porous material that was fully soaked with TiO<sub>2</sub>-water nanofluid. The undulating vertical walls of the staggered enclosure were kept at different temperatures, with one side being hot and the other side being frigid. The straight horizontal walls were regarded as both insulated and impermeable. The Galerkin Finite Element Method was employed to solve the fundamental equations, and a comprehensive description of the results was provided. Increasing the Rayleigh number and nanoparticle volume percentage resulted in enhanced heat transmission. More precisely, when the Rayleigh number was doubled, there was an 80% increase in heat transport. The maximum streamline values did, however, decrease as the nanofluid density increased. Reducing the Darcy number resulted in lower maximum streamline values and an average lower Nusselt number.

Also, for every unit increase in the heat-generating factor, the Nusselt number dropped by 30%. The ideal streamlining value was also achieved at a 60-degree inclination angle.

Liu et al. [11] conducted experimental investigations on the natural convection and entropy generation of Fe<sub>3</sub>O<sub>4</sub>-water nanofluids in cavities. They analyzed various influencing factors, such as different mass fractions and heating powers, in detail. Additionally, they combined unique square cavities with magnetic fields during their analysis. There were six square cavities with varying configurations and depths of cylindrical grooves, whereas the magnetic fields exhibited three distinct orientations and intensities. The experimental data showed that the most effective configuration for the square cavity and magnetic field was a staggered setup, with a bilateral staggered vertical intensity. The utilization of cylindrical grooves and magnetic fields has the potential to reduce thermal resistance and improve the efficiency of convection heat transfer. Enhancing heat transfer can be achieved by improving both mass fraction and heating power. Additionally, the calculation and analysis of entropy generation in the square cavity were also conducted.

In a porous cavity with a wavy form, the phenomena of hydromagnetic double diffusive mixed convection was investigated by Akhter et al. [12]. A revolving heat source and a hybrid nanofluid filled the chamber. The wavy-shaped cavity's focal point was a cylindrical heat source that revolved around it. The fluid domain inside the hollow was partially heated by the spinning heat source and the bottom wall. The finite element approach was used to quantitatively solve the governing partial differential equations. Validation of the computational method was achieved through reasonable comparisons. Results showed that, with a rotating heat source present, local entropy production, streamline circulation, and isotherms were significantly altered. The flow velocity exhibited a significant and rapid increase as the rotation speed of the cylinder increased. This increase was maximized by higher levels of cavity porosity and permeability, but limited by the impact of a magnetic field and the presence of amalgamating hybrid nanoparticles. The entropy generating components experienced a considerable impact when the physical parameters reached higher values. The Bejan number exhibited a decreasing trend across all the influential parameters that were examined.

Natural convection and entropy formation in a confined chamber were the subjects of a research by Hashemi-Tilehnoee et al. [13]. Eight packed beds, or spherical pebbles stacked in a structured manner, were confined within the chamber, which was filled with a mixture of water and Al<sub>2</sub>O<sub>3</sub>-water nanofluid. An external magnetic field and surface heat radiation were also included in the study. The numerical technique was checked by looking at two cases where conductive solid blocks and a magnetic field were present in two-dimensional cavities. When evaluating the conduction of heat in the air-filled cubical cavity, not only were two-dimensional situations considered, but also a third-dimensional one. The Hartmann number, the Rayleigh number, and the ratio of the solid-to-liquid thermal conductivity were the main variables that were taken into account. The outcomes were shared for a variety of parameters, such as the mean Nusselt number, mean Bejan number, isotherm patterns, velocity distribution, and localized entropy production. The mean Nusselt number showed a decrease of around 2% when a magnetic field was added.

Nemati and Chamkha [14] used convective heat transfer to generate entropy and studied how heat absorption and production affected non-Newtonian flow properties. We postulated the presence of mixed convection within a semi-elliptical chamber containing a power-law nanofluid in this investigation. The Brownian motion of nanoparticles was specifically considered. The cold enclosure has three different heating systems applied to its curved walls and its vertical walls. A phase difference and non-uniform distribution of velocities were observed on the chamber's vertical wall, in contrast to the cold wall's motionless state. The lattice Boltzmann method was used to simulate the flow, and by

comparing the results to previous relevant research, their correctness was validated. There is a direct relationship between the mean Nusselt number and the phase difference, according to the research results.

The authors Nouraei et al. [15] conducted a numerical simulation to study the flow of nanofluid in an open cavity under mixed convection. They specifically focused on analyzing different heat transfer zones. In order to improve the transfer of heat, water was supplemented with copper nanoparticles at varying volume percentages. The study sought to identify the most advantageous location that increases heat transfer within a circular open chamber. The investigation focused on studying the flow of nanofluid at various Reynolds values. In contrast, the high-temperature regions within the curved section of the exposed cavity were shown to be distinct in multiple instances. The findings indicated that the fluid's slow movement throughout the circular section of the cavity, particularly in the region of the hot wall, primarily facilitated natural convection driven by density variations. Furthermore, the hot sections intensified the flow circulation. The exchange was enhanced by augmenting the Reynolds number, which corresponds to the momentum term. Consequently, the temperature distribution within the cavity became more homogeneous.

The large number of parameters affecting the characteristics of nanofluid flows and the complex relationship between these parameters make heat transfer analyzes challenging. To overcome this challenge, artificial intelligence tools are used as an alternative to traditional mathematical modeling tools. Artificial neural networks (ANN) are among the models that can provide higher accuracy compared to similar tools in modeling complex and nonlinear problems [16]. A numerical study by Prince et al. [17] sought to determine the effect of different magnetic field inclination angles and Reynolds numbers on mixed convective heat and mass transfer, entropy generation in a trapezoidal enclosure with two rotating cylinders, driven by a lid. The regulating fluids employed were a variety of water-based and hybrid nanofluids with fixed solid volume fractions. We studied the impacts of SWCNT-water, Cu-water, and Al<sub>2</sub>O<sub>3</sub>-water nanofluids, as well as three other types of SWCNT-Cu-Al<sub>2</sub>O<sub>3</sub>-water hybrid nanofluids, each with a different ratio of SWCNT, Cu, and Al<sub>2</sub>O<sub>3</sub> nanoparticles to water. Through numerical simulation, the governing Navier-Stokes, thermal energy, and mass conservation equations were solved using the Galerkin weighted residual finite element approach. By utilizing an ANN to determine the optimal values for each input parameter, the best possible outcomes for the output parameters might be achieved. The developed new ANN model achieved a good level of accuracy while predicting the respective results. The model achieved an accuracy of 96.81% in predicting convective heat and mass transfer for the training and validation data. Additionally, it achieved an accuracy of 98.74% in predicting the average dimensionless temperature and Bejan number.

The purpose of the study by Reddy et al. [18] was to demonstrate the dynamics of a two-phase flow over a porous cylinder using a hybrid dusty Eyring-Powell nanofluid. The research took into account the possibility of boundary circumstances including Thompson and Troian slip. The hybrid nanofluids were made by combining ethylene glycol with a titanium alloy that is based on water. Using the Levenberg-Marquardt algorithm to regulate the feed-forward back-propagation ANN, a new approach to developing an intelligent numerical computing solution was shown. Because the velocity profile had high values, the curvature parameter was increased. Similar to how the specific heat ratio parameter exhibited an upward trend when radiation parameter values fell, temperature also rose. Increasing the values of the melting factor and velocity slip parameter caused the Nusselt number to fall.

Jery et al. [19] utilized deep learning methods to forecast the Nusselt number and quantify the overall entropy creation. The models exhibited a mean absolute error that was less than 5%. Hyperparameter tuning was conducted to identify the most precise model. The process involved fine-tuning all the parameters in the neural network to achieve optimal outcomes. The prediction models' outcomes were compared to both experimental and benchmark findings. In addition, the model's predictive capabilities were assessed using the coefficient of determination. Water and nanofluids passing through square, rectangular, and circular cross-sections may have their Nusselt numbers and total entropy production predicted with high accuracy using the proposed models. The models had a mean absolute error that did not exceed 1.33%, representing a significant accomplishment. In addition, empirical correlations were suggested for both parameters, and a double factorial optimization was executed. The findings indicated that in order to attain optimal outcomes, the Reynolds number should exceed 1600, while the concentration of nanoparticles should be maintained at 3%.

The heat and mass transfer in a hybrid nanofluid flow when it hits a cylindrical bluff-body submerged in porous media was studied by Abad et al. [20]. Homogeneous and heterogeneous chemical processes were both taken into account in the study. As part of the investigation, the Soret and Dufour effects were considered, in addition to mixed convection and local thermal non-equilibrium inside the porous medium. The computational simulation focused on the laminar flow of a hybrid nanofluid consisting of Al<sub>2</sub>O<sub>3</sub>-Cu-water in a single-phase mixture. The simulation also accounted for the coupled transport mechanisms. To address this issue, the simulation data is inputted into an ANN in order to estimate the desired outcomes. A slight change in the volume proportion of nanoparticles was shown to significantly impact the behavior of the thermal and solutal domains. Specifically, increasing the concentration of nanoparticles resulted in an augmentation in the formation of chemical species. Additionally, the technique of particle swarm optimization was utilized to forecast the relationships between Nusselt and Sherwood numbers by systematically identifying the most significant parameters.

In studies on heat transfer improvement and entropy production of nanofluids, the fact that there are many parameters affecting the outputs in question, as well as the fact that these parameters have a complex physical structure and are non-linear functional, are among the main difficulties in the studies. In the experimental determination of thermophysical properties and heat transfer parameters of nanofluids, there is another important parameter such as time, along with the financial difficulties in establishing the experimental systematics. These stated difficulties have led researchers to work on powerful simulation methods. ANNs, which have a more powerful structure than traditional mathematical tools in modeling complex physical functions, are one of the engineering tools widely used in this field. In this study, the entropy production and heat transfer characteristics of Al<sub>2</sub>O<sub>3</sub>-Cu/water hybrid nanofluid in the convection-radiation interaction flow in a porous cavity were examined with a machine learning approach. It is thought that this study, which was conducted on the prediction of these complex physical properties with high accuracy with a machine learning approach, unlike traditional mathematical tools, without the need for experimental studies, will be an important study aiming to close the gap in this field in the literature. Further recent numerical investigations continue to explore complex fluid dynamics and heat transfer phenomena in porous enclosures, including the impact of nanoparticle shape factors and non-Newtonian fluid characteristics [21,22].

## 2 Data Collection Methodology

This research's data set was sourced from a previous study by Ahmed et al. [23]. In the study conducted by Ahmed et al. [23], radiative natural transport of micropolar Al<sub>2</sub>O<sub>3</sub>-Cu/water hybrid nanofluid in a Darcy porous space was discussed. The natural convection within the square cavity

was characterized by specific thermal boundary conditions: a part of the bottom side was heated to a prescribed high temperature, while corresponding parts of the top and side walls were kept at a cooled temperature; the remaining sections of all walls were thermally insulated. The porous medium was assumed to be in thermal equilibrium, assuming that the nanoparticles and base fluid were homogeneous and all side walls were impermeable. The radiation heat flux applied in the porous space saturated with Al<sub>2</sub>O<sub>3</sub>-Cu/water hybrid nanofluid was formulated according to the Rosseland approach by Martyushev and Sheremet, and the extended Brinkman Darcy expression was adopted. Average Nusselt Number ( $Nu_{av}$ ), Bejan number ( $Be_{av}$ ) and entropy generation ( $S_{av}$ ) values obtained from the study, varying depending on the Hartmann number (Ha) and inclination ( $\phi$ ) values, are given in [Table 1](#).

**Table 1:** Data set used in the study [23]

Inputs		Outputs		
Ha	$\phi$	$Nu_{av}$	$Be_{av}$	$S_{av}$
10	0	11.5421	0.0481	2242.1680
10	45	11.5807	0.0465	2258.9230
10	90	11.6209	0.0453	2275.9250
10	135	11.5807	0.0466	2258.8320
10	180	11.5421	0.0481	2242.2020
25	0	10.9156	0.0541	1989.5330
25	45	11.1133	0.0421	2072.6100
25	90	11.3521	0.0393	2159.5280
25	135	11.1133	0.0422	2072.0630
25	180	10.9156	0.0541	1989.5330
50	0	3.7320	0.6956	108.4820
50	45	9.7638	0.0247	1632.2580
50	90	10.4317	0.0291	1825.2730
50	135	9.7638	0.0249	1631.3410
50	180	3.7320	0.6955	108.4750
100	0	3.7296	0.7936	96.3690
100	45	3.7304	0.7568	103.2940
100	90	3.7319	0.7095	112.6960
100	135	3.7303	0.7567	103.3350
100	180	3.7296	0.7936	96.3710

The numerical simulations from which the dataset was derived in Ahmed et al. [23] maintained several key parameters at fixed values while varying the Ha and  $\phi$ . These constant parameters characterize the physical system and ensure the consistency of the underlying fluid dynamics and heat transfer mechanisms. The specific fixed values of these parameters, which define the conditions under which the  $Nu_{av}$ ,  $Be_{av}$ ,  $S_{av}$  were computed, are detailed in [Table 2](#). It is important to note that while the porosity is integral to the porous medium model and the definitions of thermophoresis

and Brownian motion parameters, its specific numerical value was not explicitly reported as a fixed constant in the source's tabulated data. Similarly, while hot and cold boundary temperatures define the thermal conditions, their exact numerical values were not listed as fixed parameters; however, the temperature difference was consistently applied for the non-dimensionalization of the temperature field.

**Table 2:** Fixed parameter values from Ahmed et al. [23] for the dataset

Parameter	Symbol	Value
Rayleigh number	Ra	1.00E+06
Darcy number	Da	1.00E−03
Nanoparticle volume fraction (Al <sub>2</sub> O <sub>3</sub> )	φAl	2%
Nanoparticle volume fraction (Cu)	φCu	2%
Radiation parameter	Rd	0.1
Vortex viscosity parameter	k	1
Chemical reaction rate parameter	Kr	0.5
Heat source length (dimensionless)	B	0.4
Thermophoresis parameter	Nt	0.1
Brownian motion parameter	Nb	0.1
Buoyancy ratio parameter	Rac	1

To provide a complete understanding of the hybrid nanofluid system, the thermophysical properties of the Al<sub>2</sub>O<sub>3</sub>-Cu/water mixture, which underpin the numerical simulations of Ahmed et al. [23], are detailed here. The base fluid was water, and the nanoparticles were Al<sub>2</sub>O<sub>3</sub> and Cu, utilized at a fixed volume fraction of 2% for Al<sub>2</sub>O<sub>3</sub> (φAl) and 2% for Cu (φCu), resulting in a total solid volume concentration of 4%. The individual properties of these components were obtained from established literature and are (for water, Cu, Al<sub>2</sub>O<sub>3</sub>, respectively): density (997.1, 8933, 3970 kg/m<sup>3</sup>), specific heat (4179, 385, 765 J/kg·K), thermal conductivity (0.613, 401, 40 W/m·K), thermal expansion coefficient (21 × 10<sup>−5</sup>, 1.67 × 10<sup>−5</sup>, 0.85 × 10<sup>−5</sup> K<sup>−1</sup>), and electrical conductivity (0.05, 5.96 × 10<sup>7</sup>, 1 × 10<sup>−10</sup> S/m).

The effective thermophysical properties of the hybrid nanofluid were then calculated using standard mixing rules and correlations: the density, specific heat, and thermal expansion coefficient were determined using direct volume-weighted averages, while the effective thermal conductivity and electrical conductivity were derived from modified Maxwell models for hybrid nanofluids. The effective dynamic viscosity was calculated using the Brinkman model. It is important to note that, as specified in the source study, temperature-dependent variations in these thermophysical properties were not considered; instead, constant effective properties for the nanofluid mixture were applied throughout the numerical simulations.

### 3 ANN Model Design

The heat transfer and entropy generation characteristics of an Al<sub>2</sub>O<sub>3</sub>-Cu/water hybrid nanofluid in a porous cavity's convection-radiation interaction flow were predicted using an ANN model. In analyzing the heat transfer characteristics, Nu<sub>av</sub> and Be<sub>av</sub> values, which are important characteristic parameters, were discussed. In the developed ANN model, multilayer perceptron (MLP) architecture, which is one of the models that can provide high prediction performance due to its strong structural

features, was used [24].  $Ha$  and  $\phi$  values were defined as input parameters in the input layer of the MLP network, which consists of three basic layers, and  $Nu_{av}$ ,  $Be_{av}$  and  $S_{av}$  values were gained in the output layer. The structural configuration of the developed MLP network model is given in Fig. 1.

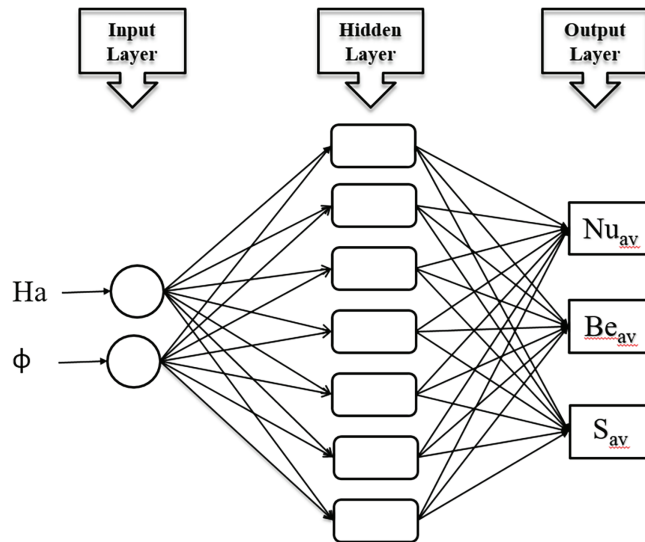


**Figure 1:** The structural configuration of the developed MLP network model

When building ANN models, it's best to combine the data sets together [25]. Out of the twenty data sets used to build the ANN, fifteen were utilized for training and five for validation. In MLP networks, the amount of neurons employed in the hidden layers is determined in an *ad hoc* fashion [26]. For small datasets, alternative validation strategies such as k-fold cross-validation or leave-one-grid-point-out validation, particularly relevant for datasets derived from a structured grid of input parameters, offer a more robust assessment of model generalization by averaging performance over multiple data partitions. These methods help to mitigate the risk of an unrepresentative validation set and provide a more comprehensive understanding of the model's predictive reliability across the entire data range.

A network model with 10 hidden layer neurons developed after comparing its prediction performance to those with varying numbers of neurons. Fig. 2 displays the fundamental structural elements of the created MLP network.

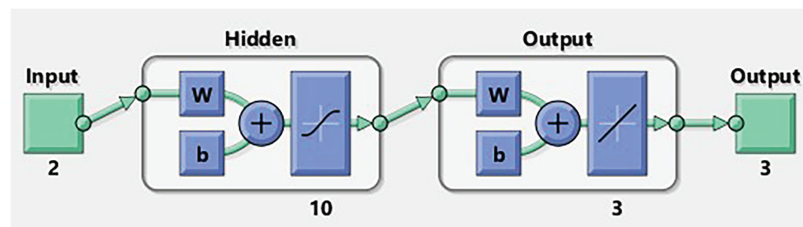


**Figure 2:** The basic structural features of the developed MLP network

The training technique for the network model was the Bayesian Regularization algorithm, and the transfer function was the hyperbolic tangent sigmoid. The hyperbolic tangent sigmoid transfer

function is mathematically expressed as follows [27]:

$$\text{TanSig}(n) = \frac{2}{1 + e^{(-2n)}} - 1 \quad (1)$$

A number of performance metrics with a strong literature presence were identified in order to assess the created ANN model's prediction capabilities. The mathematical formulae that were utilized to determine the values of the performance parameters—the coefficient of determination (R), mean squared error (MSE), and margin of deviation (MoD)—are shown below [28]:

$$R = \sqrt{1 - \frac{\sum_{i=1}^N (X_{\text{targ}(i)} - X_{\text{pred}(i)})^2}{\sum_{i=1}^N (X_{\text{targ}(i)})^2}} \quad (2)$$

$$\text{MSE} = \frac{1}{N} \sum_{i=1}^N (X_{\text{targ}(i)} - X_{\text{pred}(i)})^2 \quad (3)$$

$$\text{MoD} (\%) = \left[ \frac{X_{\text{pred}} - X_{\text{pred}}}{X_{\text{targ}}} \right] \times 100 \quad (4)$$

#### 4 Results and Discussion

Along with the developments in the field of nanotechnology, the critical roles of nanofluids have led to an increase in research in this field. Many applications have been developed with these technological developments in the field of energy, fluid mechanics and heat transfer. Since increasing energy efficiency is an important parameter in financial and environmental terms, studies in the heat transfer field of nanotechnology have focused on improving heat transfer. In this context, the issue of heat transfer in flows in porous cavities has been among the important topics such as microchip cooling, heat exchangers and solar energy applications.

Al<sub>2</sub>O<sub>3</sub>-Cu/water hybrid nanofluid is considered for convection-radiation interaction flow in a porous space. Nu<sub>av</sub> and Be<sub>av</sub> parameters and S<sub>av</sub> values, which are heat transfer characteristics of nanofluid flow, were analyzed numerically. Nanofluid flow and heat transfer rate are enhanced by the radiation parameter, but angular velocity is supported and convective flow is reduced by the vortex parameter. No matter what the regulating factors are, heat transport is paramount close to the active components. Within extended warm regions, both the local and average Nusselt numbers diminish. As the volume fractions of Al<sub>2</sub>O<sub>3</sub> and Cu increase, the entropy generation ratio to the average Nusselt ratio drops. A magnetic field reduces the average and local Nusselt numbers and weakens the flow.

A comparison between the goal values and the ANN model's output values for Nu<sub>av</sub> and Be<sub>av</sub>, and S<sub>av</sub> was the initial step in analyzing the model's prediction performance. The results of comparing each parameter based on the data points used to create the ANN models are shown in Fig. 3. The data points depicting the goal values and the data points representing the ANN model's outputs are very congruent, as can be observed by looking at Fig. 3. The created ANN model can predict Nu<sub>av</sub> and Be<sub>av</sub>, and S<sub>av</sub> values with high accuracy, as shown by the excellent fit achieved for each data point. The created ANN model may give extremely high prediction accuracy, since the R value is near to 1. An additional performance metric, the MSE, was found to be 6.38E-05. The network model is able to produce predictions with little mistakes, as seen by the low MSE value. The acquired data conclusively demonstrate that the created ANN model is capable of making extremely accurate predictions of Nu<sub>av</sub> and Be<sub>av</sub>, and S<sub>av</sub> values. A detailed analysis of the Be<sub>av</sub> values, which indicate the relative dominance of

heat transfer irreversibility, reveals important trends within the dataset. All  $Be_{av}$  values, consistently fall within the physically expected range of 0 to 1, underscoring the model's adherence to thermodynamic principles.

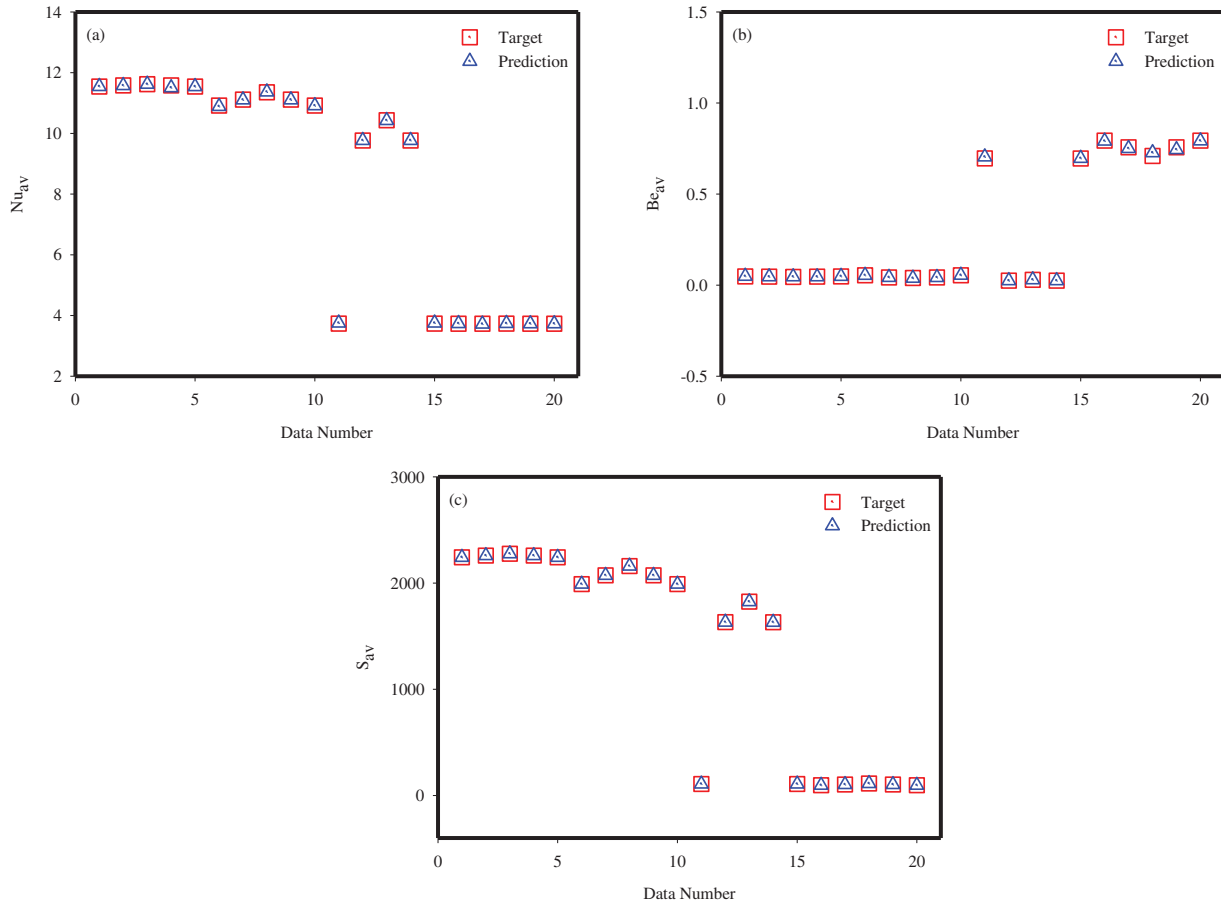


**Figure 3:** The comparison results for each parameter according to the data number (a) for  $Nu_{av}$ , (b) for  $Be_{av}$  and (c) for  $S_{av}$

For  $Ha$  of 10, 25, and 100, the  $Be_{av}$  generally exhibits a symmetric, U-shaped periodic behavior with respect to the  $\phi$ , with values decreasing from  $0^\circ$  to  $90^\circ$  and then increasing towards  $180^\circ$ . This behavior aligns with the general periodic behaviors noted in the source study and suggests a systematic influence of magnetic field orientation on the balance of irreversibilities. Furthermore, at constant  $\phi = 0^\circ$  or  $180^\circ$ ,  $Be_{av}$  generally increases with increasing  $Ha$ , indicating that a stronger magnetic field tends to enhance the relative dominance of heat transfer irreversibility under these aligned conditions, as physically interpreted in Ahmed et al. [23]. However, a distinct and non-monotonic trend is observed specifically at  $Ha = 50$ . For this Hartmann number, the  $Be_{av}$  values dramatically decrease from 0.6956 at  $\phi = 0^\circ$  to 0.0247 at  $\phi = 45^\circ$ , slightly increase to 0.0291 at  $\phi = 90^\circ$ , then decrease to 0.0249 at  $\phi = 135^\circ$ , and finally sharply increase back to 0.6955 at  $\phi = 180^\circ$ . This significant drop in  $Be_{av}$  at intermediate inclination angles ( $45^\circ$ ,  $90^\circ$ ,  $135^\circ$ ) at  $Ha = 50$  suggests a substantial shift where the irreversibility due to fluid friction or other magnetic effects becomes relatively more prominent than heat transfer irreversibility, in stark contrast to the trends seen at other  $Ha$  values. Additionally, when examining the

trend of  $Be_{av}$  with increasing  $Ha$  at fixed intermediate angles (e.g.,  $\phi = 45^\circ$  or  $90^\circ$ ), a non-monotonic ‘dip’ is observed at  $Ha = 50$ , where  $Be_{av}$  decreases from lower  $Ha$  values before increasing significantly at  $Ha = 100$ . This complex, non-linear response highlights the intricate coupling between magnetic field strength, its orientation, and the resulting entropy generation mechanisms in hybrid nanofluid flows. The high accuracy of the ANN model in predicting  $Be_{av}$ , with an average deviation rate of  $-0.11\%$ , confirms its capability to faithfully reproduce these nuanced and physically significant non-monotonic trends present in the original numerical data.

Eq. (4) was used to determine the deviation rates between the goal values for each data point and the  $Nu_{av}$  and  $Be_{av}$ , and  $S_{av}$  values produced by the ANN model. This allowed us to assess the prediction mistakes of the ANN model. Upon closer inspection of the data points representing the deviation rates for each of the  $Nu_{av}$  and  $Be_{av}$ , and  $S_{av}$  values in Fig. 4, it becomes apparent that they are often situated near the zero deviation line.

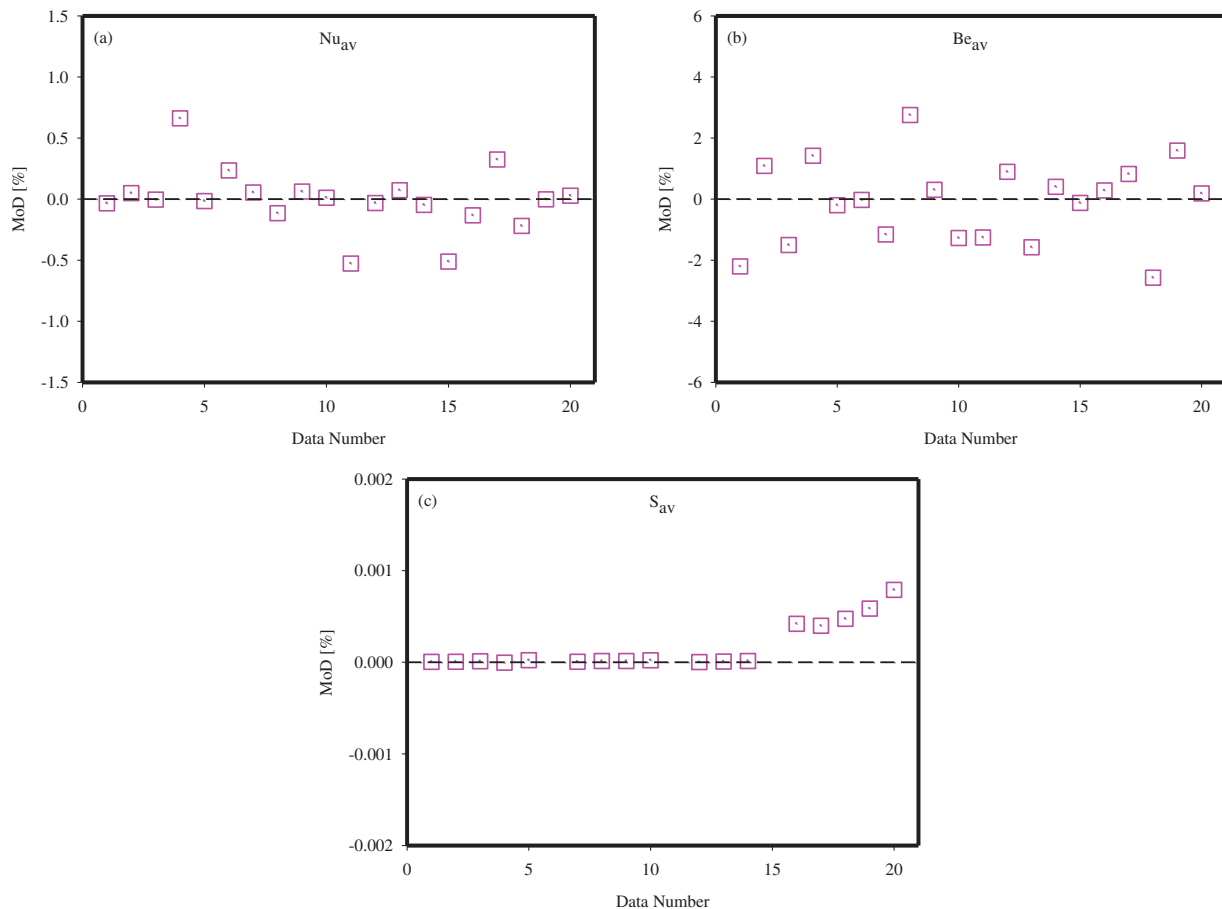


**Figure 4:** MoD values calculated according to data number (a) for  $Nu_{av}$ , (b) for  $Be_{av}$  and (c) for  $S_{av}$

$Nu_{av}$  and  $Be_{av}$ , and  $S_{av}$  values have average deviation rates of  $-0.007\%$ ,  $-0.11\%$ , and  $0.0002\%$ , correspondingly. The created ANN model can predict  $Nu_{av}$  and  $Be_{av}$ , and  $S_{av}$  values with extremely low errors, according to these results acquired from deviation rates. For a more thorough error analysis of the created ANN model, we computed, for each data point, the discrepancies between the actual  $Nu_{av}$  and  $Be_{av}$ , and  $S_{av}$  values and the ANN model’s  $Nu_{av}$ ,  $Be_{av}$ , and  $S_{av}$  values. As can be seen from the

graphs provided for each data point in Fig. 5, the computed error values for the  $Nu_{av}$  and  $Be_{av}$ , and  $S_{av}$  parameters are rather small. The created ANN model can predict the  $Nu_{av}$  and  $Be_{av}$ , and  $S_{av}$  values with extremely low errors, as further evidenced by the low errors between the values acquired from the model and the target values.

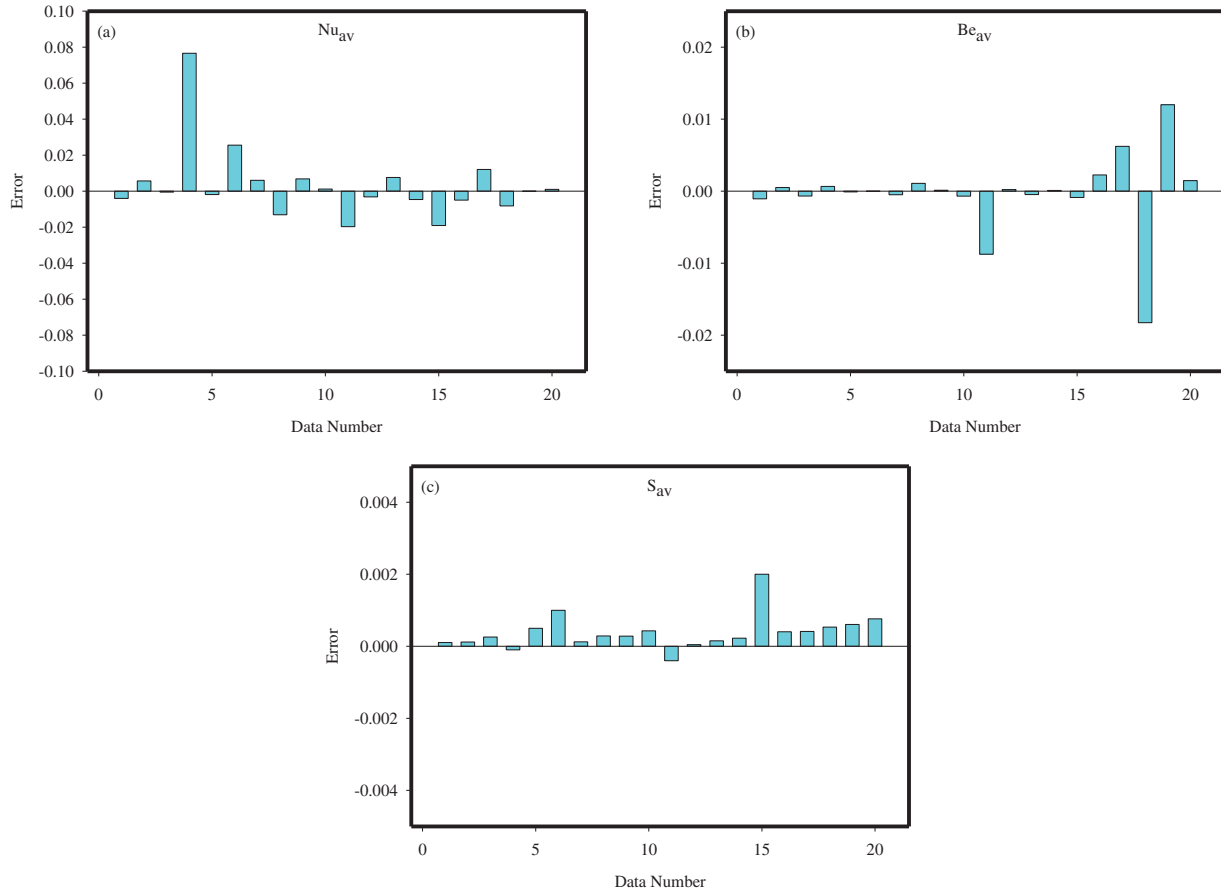


**Figure 5:** The differences between the real values and the values obtained from the ANN model (a) for  $Nu_{av}$ , (b) for  $Be_{av}$  and (c) for  $S_{av}$

Fig. 6 shows the goal  $Nu_{av}$  and  $Be_{av}$ , and  $S_{av}$  values on the  $x$ -axis and the ANN model's output on the  $y$ -axis. Analysis of the acquired data points reveals that, in the vast majority of cases, they lie on the zero error line. The created ANN model yielded an R-value of 0.99999.

While the developed ANN model exhibits exceptional accuracy in predicting the  $Nu_{av}$ ,  $Be_{av}$ , and entropy generation for the specific  $Ha$  and  $\phi$  combinations present in the original dataset, it is important to acknowledge that explicit interpolation or extrapolation tests on unseen data points were not performed within this study. The model's generalization capability to predict outcomes for novel, intermediate (interpolated) or slightly outside (extrapolated)  $Ha/\phi$  combinations, such as  $Ha = 75$  and  $\phi = 30^\circ$ , has not yet been rigorously assessed. Such comprehensive testing, particularly given the discrete nature of the foundational numerical data, would further validate the model's robustness and its broader applicability in scenarios where the exact operational parameters may differ from the

training instances. This remains a significant avenue for future research to enhance the practical utility and confidence in the ANN's predictive power across a continuous parameter space.

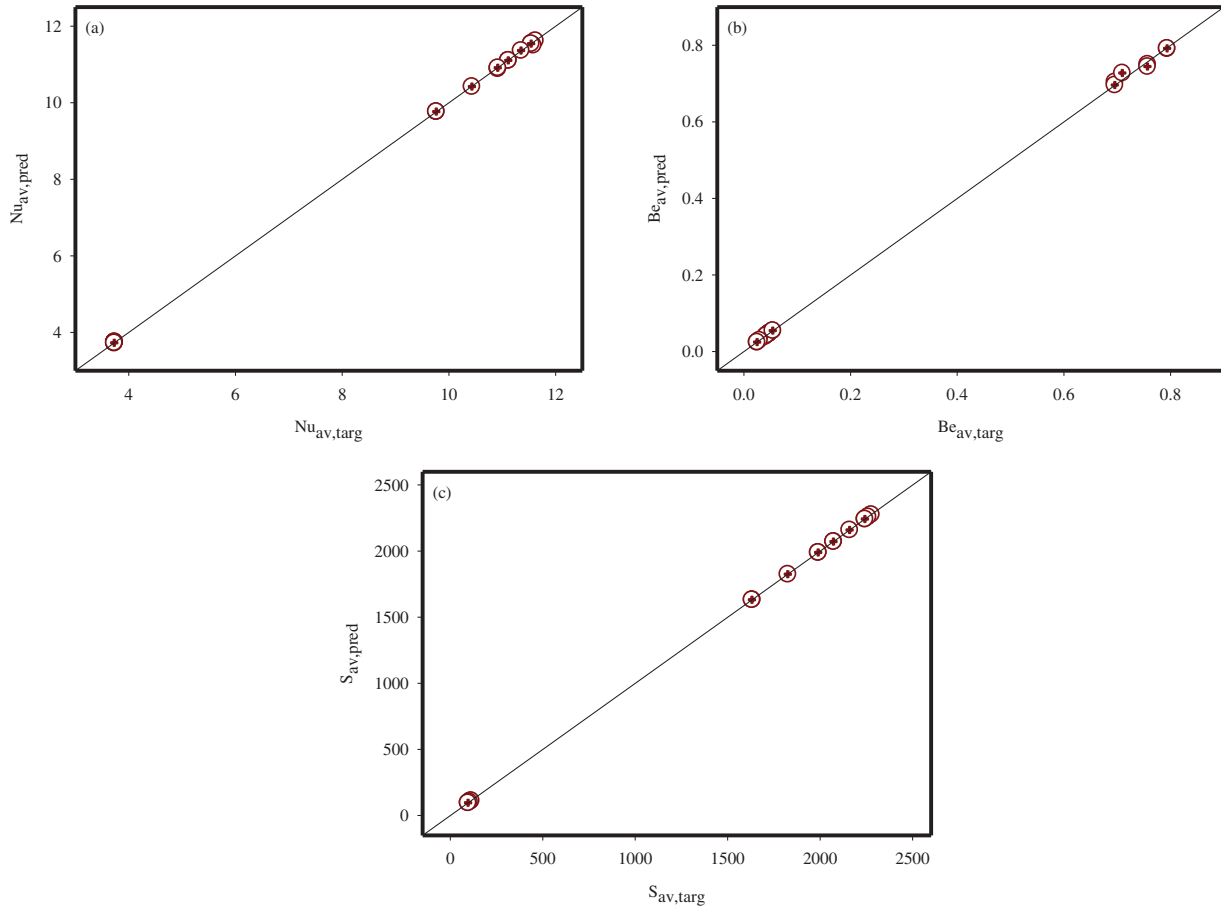


**Figure 6:** The  $Nu_{av}$ ,  $Be_{av}$  and  $S_{av}$  values obtained from the ANN model and the target values (a) for  $Nu_{av}$ , (b) for  $Be_{av}$  and (c) for  $S_{av}$

While the Bayesian Regularization algorithm, utilized for training, provides a robust framework for model development by incorporating regularization to improve generalization, this study did not explicitly quantify the predictive uncertainty through the generation of prediction intervals or confidence bounds. Providing such intervals, derived perhaps through methods like bootstrapping or a more direct Bayesian inference approach, would offer a comprehensive understanding of the model's reliability beyond point estimates. This would enable users to gauge the confidence associated with each prediction, which is particularly valuable when the model is applied to unseen data or to conditions slightly outside the training range. Incorporating uncertainty quantification in future research will further enhance the practical applicability and interpretability of the developed ANN model.

A detailed physical interpretation of the results, particularly concerning the influence of the  $Ha$  and  $\phi$  on the  $Nu_{av}$ ,  $Be_{av}$ , and  $S_{av}$ , is crucial for understanding the underlying thermofluidic phenomena. As observed from the original numerical simulations, the  $Ha$ , which quantifies the strength of the magnetic field, significantly impacts these characteristics. An increase in  $Ha$  generally leads to a reduction in the  $Nu_{av}$  and total  $S_{av}$ . This behavior is primarily attributed to the Lorentz force exerted by

the magnetic field, which acts as a resistive force, thereby suppressing the fluid motion and weakening the convective heat transfer. The diminished convective currents also contribute to a reduction in the overall irreversibility within the system. Conversely, the  $Be_{av}$  typically increases with rising  $Ha$ . This indicates that, despite a potential decrease in total entropy generation, the irreversibility associated with heat transfer becomes relatively more dominant compared to other sources of irreversibility, such as fluid friction or magnetic field effects, at higher magnetic field strengths.

The  $\phi$ , which dictates the orientation of the magnetic field, also plays a critical role. The numerical data reveals periodic behaviors for  $Nu_{av}$ ,  $Be_{av}$ , and  $S_{av}$  as  $\phi$  varies from  $0^\circ$  to  $180^\circ$ . This periodicity is a direct consequence of how the magnetic field's orientation alters the components of the Lorentz force, thus influencing the flow patterns and the balance between different entropy generation mechanisms in a cyclical manner. A particularly notable observation is the non-monotonic trend of  $Be_{av}$  at  $Ha = 50$ , where  $Be_{av}$  experiences a substantial decrease at intermediate inclination angles ( $45^\circ$ ,  $90^\circ$ ,  $135^\circ$ ) before recovering at  $0^\circ$  and  $180^\circ$ . This sharp decline suggests a shift in the dominant source of irreversibility, implying that at these specific conditions, fluid friction or magnetic irreversibility becomes relatively more significant than heat transfer irreversibility. The exceptional predictive accuracy of the ANN model across all parameters, with an R-value of 0.99999 and minimal deviation rates, underscores its ability to precisely capture these complex, non-linear, and physically significant interdependencies between the magnetic field parameters and the thermofluidic characteristics of the hybrid nanofluid.

## 5 Conclusion

The main challenges in studies on heat transfer improvement and entropy production of nanofluids arise from the numerous parameters that influence the desired outcomes. Additionally, these parameters possess a complex physical structure and exhibit non-linear functionality. When conducting experiments to determine the thermophysical characteristics and heat transfer parameters of nanofluids, it is vital to consider the parameter of time, in addition to the challenges of establishing the experimental systematics due to financial constraints. These aforementioned challenges have prompted academics to develop robust simulation techniques. ANNs, being a superior framework compared to conventional mathematical instruments for representing intricate physical functions, are extensively employed as engineering tools in this domain. This work scrutinized the entropy production and heat transfer properties of a hybrid nanofluid consisting of Al<sub>2</sub>O<sub>3</sub>-Cu particles suspended in water. The nanofluid was subjected to convection-radiation interaction flow within a porous cavity. A machine learning method was employed to analyze the data. An ANN model was developed to predict  $Nu_{av}$ ,  $Be_{av}$  and  $S_{av}$  values depending on  $Ha$  and  $\phi$  values. In the network model that was trained using a total of 20 data sets, 15 of the data were used for training the model and 5 for the testing phase. There are 10 neurons in the hidden layer of the network model with MLP architecture. TanSig transfer function was used in the network model trained with the Bayesian Regularization training algorithm. The  $Nu_{av}$ ,  $Be_{av}$  and  $S_{av}$  values obtained from the ANN model were compared with the target values and it was seen that both data were in perfect harmony. The established ANN model was able to predict  $Nu_{av}$ ,  $Be_{av}$  and  $S_{av}$  values with average deviation rates of  $-0.007\%$ ,  $-0.11\%$  and  $0.0002\%$ , respectively. Among the performance parameters used for the performance analysis of the ANN model, the R value was calculated as 0.99999 and the MSE value was  $6.38E-05$ . All these results have shown that the developed ANN model can predict  $Nu_{av}$ ,  $Be_{av}$  and  $S_{av}$  values with very high accuracy.

Beyond its exceptional predictive accuracy, the developed ANN surrogate model possesses significant practical value for engineering applications. By providing rapid and reliable predictions for the average  $Nu_{av}$ ,  $Be_{av}$ , and  $S_{av}$  based on the  $Ha$  and  $\phi$ , this model offers a powerful alternative

to time-consuming and resource-intensive numerical simulations or experimental studies. Its utility lies in facilitating accelerated design and optimization processes for thermal systems utilizing hybrid nanofluids in porous cavities. For instance, in the design of efficient cooling systems or heat exchangers, engineers can embed this surrogate model to quickly identify optimal magnetic field strengths and orientations that maximize heat transfer while minimizing entropy production, thereby enhancing overall system efficiency and reducing operational costs. This ability to perform instantaneous “what-if” analyses across a broad parameter space positions the ANN model as a valuable tool for informed decision-making in both research and industrial contexts, bridging the gap between complex physical phenomena and practical engineering solutions.

**Acknowledgement:** This study was conducted using the data existing in the study published by Ahmed et al. [23]. The author would like to thank Ahmed et al. [23] for their contributions.

**Funding Statement:** The author received no specific funding for this study.

**Availability of Data and Materials:** No Data associated in the manuscript.

**Ethics Approval:** Not applicable.

**Conflicts of Interest:** The author declares no conflicts of interest to report regarding the present study.

## References

1. Aglawe KR, Yadav RK, Thool SB. Preparation, applications and challenges of nanofluids in electronic cooling: a systematic review. *Mater Today Proc.* 2021;43:366–72. doi:10.1016/j.matpr.2020.11.679.
2. Abbas F, Ali HM, Shah TR, Babar H, Janjua MM, Sajjad U, et al. Nanofluid: potential evaluation in automotive radiator. *J Mol Liq.* 2020;297:112014. doi:10.1016/j.molliq.2019.112014.
3. Tarafdar A, Sirohi R, Negi T, Singh S, Badgajar PC, Chandra Shahi N, et al. Nanofluid research advances: preparation, characteristics and applications in food processing. *Food Res Int.* 2021;150(3):110751. doi:10.1016/j.foodres.2021.110751.
4. Hussein AK. Applications of nanotechnology to improve the performance of solar collectors-recent advances and overview. *Renew Sustain Energy Rev.* 2016;62:767–92. doi:10.1016/j.rser.2016.04.050.
5. Alnarabiji MS, Husein MM. Application of bare nanoparticle-based nanofluids in enhanced oil recovery. *Fuel.* 2020;267:117262. doi:10.1016/j.fuel.2020.117262.
6. Krishna MV, Chamkha AJ. Hall and ion slip effects on Unsteady MHD convective rotating flow of nanofluids—application in biomedical engineering. *J Egypt Math Soc.* 2020;28(1):1. doi:10.1186/s42787-019-0065-2.
7. Hatami M, Domairry G, Mirzababaei SN. Experimental investigation of preparing and using the H<sub>2</sub>O based nanofluids in the heating process of HVAC system model. *Int J Hydrog Energy.* 2017;42(12):7820–5. doi:10.1016/j.ijhydene.2016.12.104.
8. Bejan A. The concept of irreversibility in heat exchanger design: counterflow heat exchangers for gas-to-gas applications. *J Heat Transf.* 1977;99(3):374–80. doi:10.1115/1.3450705.
9. Jiang X, Hatami M, Abderrahmane A, Younis O, Makhdom BM, Guedri K. Mixed convection heat transfer and entropy generation of MHD hybrid nanofluid in a cubic porous cavity with wavy wall and rotating cylinders. *Appl Therm Eng.* 2023;226:120302. doi:10.1016/j.applthermaleng.2023.120302.
10. Al-Amir QR, Hamzah HK, Ali FH, Hatami M, Al-Kouz W, Al-Manea A, et al. Investigation of natural convection and entropy generation in a porous titled Z-staggered cavity saturated by TiO<sub>2</sub>-water nanofluid. *Int J Thermofluids.* 2023;19:100395. doi:10.1016/j.ijft.2023.100395.

11. Liu Y, Tian Z, Qi C, Li R. Natural convection and entropy generation of Fe<sub>3</sub>O<sub>4</sub>-H<sub>2</sub>O nanofluids in square cavities with cylindrical grooves under magnetic field. *Colloids Surf A Physicochem Eng Asp.* 2023;679:132564. doi:10.1016/j.colsurfa.2023.132564.
12. Akhter R, Ali MM, Alim MA. Magnetic field impact on double diffusive mixed convective hybrid-nanofluid flow and irreversibility in porous cavity with vertical wavy walls and rotating solid cylinder. *Results Eng.* 2023;19:101292. doi:10.1016/j.rineng.2023.101292.
13. Hashemi-Tilehnoee M, Seyyedi SM, Palomo del Barrio E, Sharifpur M. Analysis of natural convection and the generation of entropy within an enclosure filled with nanofluid-packed structured pebble beds subjected to an external magnetic field and thermal radiation. *J Energy Storage.* 2023;73:109223. doi:10.1016/j.est.2023.109223.
14. Nemati M, Chamkha AJ. Examination of effective strategies on changing the amount of heat transfer and entropy during non-Newtonian magneto-nanofluid mixed convection inside a semi-ellipsoidal cavity. *J Magn Magn Mater.* 2023;578:170652. doi:10.1016/j.jmmm.2023.170652.
15. Nouraei S, Anvari A, Abed AM, Ali Akbari O, Montazerifar F, Baghaei S, et al. Heat transfer and entropy analysis for nanofluid flow in a semi-circular open cavity under mixed convection. *Alex Eng J.* 2023;64:309–34. doi:10.1016/j.aej.2022.09.007.
16. Bahiraei M, Heshmatian S, Moayedi H. Artificial intelligence in the field of nanofluids: a review on applications and potential future directions. *Powder Technol.* 2019;353:276–301. doi:10.1016/j.powtec.2019.05.034.
17. Prince HA, Ghosh A, Siam MMH, Mamun MAH. AI predicts MHD double-diffusive mixed convection and entropy generation in hybrid-nanofluids for different magnetic field inclination angles by ANN. *Int J Thermofluids.* 2023;19:100383. doi:10.1016/j.ijft.2023.100383.
18. Reddy SRR, Jakeer S, Sathishkumar VE, Basha HT, Cho J. Numerical study of TC4-NiCr/EG+Water hybrid nanofluid over a porous cylinder with Thompson and Troian slip boundary condition: artificial neural network model. *Case Stud Therm Eng.* 2024;53:103794. doi:10.1016/j.csite.2023.103794.
19. Jery AE, Ramírez-Coronel AA, Gavilán GCO, Al-Ansari N, Sammen SS. Proposing empirical correlations and optimization of Nu and Sgen of nanofluids in channels and predicting them using artificial neural network. *Case Stud Therm Eng.* 2023;45:102970. doi:10.1016/j.csite.2024.104246.
20. Abad JMN, Alizadeh R, Fattahi A, Doranehgard MH, Alhajri E, Karimi N. Analysis of transport processes in a reacting flow of hybrid nanofluid around a bluff-body embedded in porous media using artificial neural network and particle swarm optimization. *J Mol Liq.* 2020;313:113492. doi:10.1016/j.molliq.2020.113492.
21. Rajeswari VR, Venkatadri K, Prasad VR. Nanoparticle shape factor impact on double diffusive convection of Cu-water nanofluid in trapezoidal porous enclosures: a numerical study. *Numer Heat Transf Part A Appl.* 2024:1–20. doi:10.1080/10407782.2024.2380814.
22. Venkatadri K, Devi TS, Shobha A, Sekhar KR, Rajeswari VR. Numerical study of natural convection flow in a square porous enclosure filled with casson viscoelastic fluid. *Contemp Math.* 2023;4(3):279–391. doi:10.37256/cm.4320232913.
23. Ahmed SE, Mansour MA, Mahdy A. Analysis of natural convection-radiation interaction flow in a porous cavity with Al<sub>2</sub>O<sub>3</sub>-Cu water hybrid nanofluid: entropy generation. *Arab J Sci Eng.* 2022;47(12):15245–59. doi:10.1007/s13369-021-06495-6.
24. Wang J, Ayari MA, Khandakar A, Chowdhury MEH, Uz Zaman SA, Rahman T, et al. Estimating the relative crystallinity of biodegradable polylactic acid and polyglycolide polymer composites by machine learning methodologies. *Polymers.* 2022;14(3):527. doi:10.3390/polym14030527.
25. Çolak AB. An experimental study on the comparative analysis of the effect of the number of data on the error rates of artificial neural networks. *Int J Energy Res.* 2021;45(1):478–500. doi:10.1002/er.5680.
26. Çolak AB. Modeling the influence of nanoparticles and gyrotactic microorganisms on natural convection in a heated square cavity using artificial neural network (ANN). *Heat Trans Res.* 2024;55(14):1–10. doi:10.1615/heattransres.2024049994.

27. Souayeh B, Sabir Z. Designing hyperbolic tangent sigmoid function for solving the williamson nanofluid model. *Fractal Fract.* 2023;7(5):350. doi:10.3390/fractalfract7050350.
28. Çolak AB. Advancing nanofluid technology: experimental thermal conductivity measurements and accurate predictive models for yttrium oxide-water nanofluid using neural networks and mathematical correlations. *Numer Heat Transf Part B Fundam.* 2025;86(4):998–1017. doi:10.1080/10407790.2023.2300691.